

Photoassociative Ionization of Heteronuclear Molecules in a Novel Two-Species Magneto-optical Trap

J. P. Shaffer,* W. Chalupczak, and N. P. Bigelow

*Department of Physics and Astronomy and Laboratory for Laser Energetics,
The University of Rochester, Rochester, New York 14627*

(Received 26 June 1998)

We describe the experimental observation of ultracold NaCs^+ molecular formation in a novel two-species magneto-optical trap. We interpret our observations in terms of a photoassociative ionization pathway similar to that observed in a sodium trap: $\text{Na} + \text{Cs} + \hbar\omega_{\text{Na}} + \hbar\omega_{\text{Cs}} \rightarrow \text{NaCs}^+ + e^-$. We have directly measured the NaCs^+ production rate as a function of the excitation laser frequency and intensity elucidating the role of ground-state hyperfine levels. We have observed resonance structures in the frequency-dependent ion rate which we associate with the molecular character of the process. [S0031-9007(98)08234-9]

PACS numbers: 33.80.Ps

Photoassociative (PA) and photoassociative ionization (PAI) spectroscopy of laser cooled and trapped alkali atoms has recently provided [1] remarkably detailed information about long-range interatomic potentials, scattering lengths [2], and excited-state radiative lifetimes. Until recently, collisions of ultracold *heteronuclear* atomic vapors have been unexplored [3,4].

Ultracold heteronuclear PA and PAI is fundamentally different from its homonuclear counterpart for many reasons. One particularly important difference is that the interaction of a ground-excited-state heteronuclear pair lacks the long-range resonant dipole contribution ($V \sim C_3/R^3$) which plays a decisive role in the homonuclear case [5]. Instead, the long-range part of the heteronuclear pair potential is generally dominated by a comparatively shorter range interaction ($V \sim C_6/R^6$ or C_8/R^8 , for example). One consequence of this difference is that the absorption of the photoassociating photon occurs at a much smaller internuclear spacing (R_{ex}) for a heteronuclear as compared to a homonuclear pair. In PAI of Na in a magneto-optical trap (MOT) $R_{\text{ex}} \sim 1800a_0$, whereas for Na + Cs we estimate $R_{\text{ex}} \sim (40-100)a_0$ (see Table I).

The particular system under study is a vapor of cesium and sodium atoms contained in a novel two-species MOT [3]. The trapping laser beams contain two wavelengths $\lambda_{\text{Na}} = 589$ nm and $\lambda_{\text{Cs}} = 852$ nm (frequency stability ~ 1 MHz). The Na trap laser is detuned by $\Delta_{\text{Na}} = -13$ MHz ($= -1.3\Gamma_{\text{Na}}$) from the $3S_{1/2}(F=2) \rightarrow 3P_{3/2}(F'=3)$ Na $D2$ transition. Before being sent to the trap, the 589 nm light is passed through an electro-optic modulator which generates repumping sidebands shifted from the input laser frequency by ± 1.71 GHz. The intensity of each sideband is 10% of the total intensity. The 852 nm light is detuned by $\Delta_{\text{Cs}} = -23$ MHz ($= -4.4\Gamma_{\text{Cs}}$) from the $6S_{1/2}(F=4) \rightarrow 6P_{3/2}(F'=5)$ Cs $D2$ transition. Cs repumping light is provided by a frequency stabilized diode laser tuned to the $F=3 \rightarrow F'=4$ transition. The magnetic field gradient was 20 G/cm and the background pressure was $\sim 10^{-10}$ Torr.

To determine the number of trapped atoms, fluorescence from each species was isolated with narrow band ($\Delta\lambda = 9$ nm) interference filters and measured with independent, calibrated photomultipliers. Trap sizes were measured with two CCD cameras (spatial resolution $\ll 30$ μm) oriented so that complete overlap of the Cs and Na clouds could be assured in three dimensions. The production rate of positive ions was measured with a channel electron multiplier (CEM). In the absence of the MOT the ion count rate was ~ 15 Hz.

We first characterized the MOT with one species confined and verified that each single-species MOT was well behaved: Individual trapped atom densities were $\sim 10^{10}$ cm^{-3} with $\sim 10^6$ Na atoms and $\sim 10^7$ Cs atoms. Measured trap loss rate coefficients were consistent with accepted values [6]. Measurements were also made with and without opening the source for the other species and no significant changes were observed. We also measured the pure Na trap PAI rate coefficient K_{PAI} which was in excellent agreement with reported values [7].

When both species were confined, several effects were observed: First, the rate of ion production increased by

TABLE I. Long-range potential parameters for Hund's case (c) states. C_6 , C_8 , and R_{ex} are in a.u., $H_n^{2n/(n-2)}$ is in MHz.

	Movre and Beuc			Bussery <i>et al.</i>			
	C_6	$H_n^{2n/(n-2)}$	R_{ex}	C_6	C_8	$H_n^{2n/(n-2)}$	R_{ex}
CsNa*							
0 ⁺	942	N.A.	102	-1969	-1446610	N.A.	37
0 ⁻	483	N.A.	100	-101	-2516205	2886	29
1	782	N.A.	101	-3405	-560126	672	72
1	-2650	761	69	132	-2360973	2948	27
2	-2470	789	73	-3303	-416500	682	69
NaCs*							
0 ⁺	-14930	321	135	-19504	-2884437	281	143
0 ⁻	-14950	321	135	-19522	-2884930	281	143
1	-14940	321	135	-19511	-2884549	281	143
1	-7835	443	116	-10887	389711	376	126
2	-7830	443	116	-10881	389800	376	126

over 1 order of magnitude; second, the number and density of trapped Na atoms decreased markedly; third, the two-species Cs number density remained approximately unchanged. In the present paper, we focus on ion production. Other trap loss mechanisms are the subject of a separate investigation.

In Fig. 1 we show the time-of-flight (TOF) ion mass spectra made by extinguishing ($t = 0$) the Na trapping light using an acousto-optic (AO) modulator. After residual ions were swept out of the trap ($t \sim 5 \mu\text{s}$), the ion rate dropped to the background level. At $t = 20 \mu\text{s}$ the Na laser was pulsed on for 100 ns producing an ion burst. The observed ion pulse was ~ 100 ns wide and is not limited by the spatial extent of the atom cloud. Three spectra are shown in Fig. 1: (a) the Na + Cs MOT, (b) a Cs MOT, and (c) a Na MOT. The TOF spectra in (a) shows two distinct peaks corresponding to Na_2^+ and to NaCs^+ ions. To verify the mass calibration we carried out an experiment in which we produced Cs^+ ions via a two-color process in a pure Cs trap [8]. This Cs^+ mass peak is shown in TOF (b), confirming our identification of NaCs^+ in (a). By comparing the Na_2^+ production rate of the Na-only MOT (higher Na density) with that of the Na + Cs MOT (lower Na density, as noted above), we found that the lower Na_2^+ production in the Na + Cs MOT was due to the decrease in Na density.

We eliminated the possibility that the NaCs^+ was produced by background atoms. When one of the traps was quenched, the ion signal returned to the appropriate background level: We (1) eliminated the repumper only, (2) detuned the trap light to $\Delta > 10\Gamma$ (inoperative trap), or (3) blocked one of the trapping beams. In each case, only Cs or Na atoms and ions were observed, and a normal single-species trap was recovered. We conclude that NaCs^+ is due solely to collisions involving trapped Na and Cs atoms.

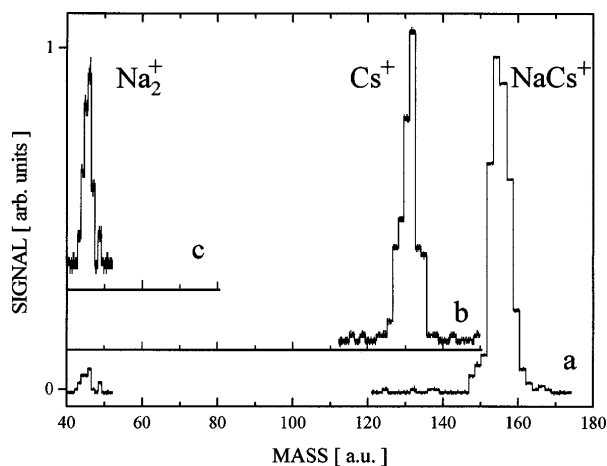


FIG. 1. Time-of-flight ion spectra (a) from the Na + Cs MOT; (b) from a Cs MOT (see [8]); (c) from a Na MOT.

We next investigated the NaCs^+ production as a function of laser intensity. This experiment was carried out in a manner similar to the TOF: Either the Cs or the Na trap laser, being held at a fixed intensity and detuning, was extinguished for $\sim 20 \mu\text{s}$, during which a $5 \mu\text{s}$ probe pulse of variable intensity induced the production of NaCs^+ (repetition rate ~ 1 kHz). The probe light was derived from a separate laser tuned to the same frequency as the extinguished trap light. We found that the NaCs^+ production depended linearly on the probe intensity up to $I \sim 100 \text{ mW/cm}^2$ for Na and $I \sim 25 \text{ mW/cm}^2$ for Cs. We conclude that the production of NaCs^+ requires one 852 nm photon and one 589 nm photon. By using a pulsed technique we ensured that the number, density, and temperature of the trapped atom sample were independent of the probe parameters. Another important feature of a pulsed approach is that NaCs^+ ions can be selectively detected via their arrival time using TOF.

We conclude that NaCs^+ is produced via two pathways similar to those used to describe PAI in pure trapped Na [9]: $\text{Na}(3S) + \text{Cs}(6S) + \hbar\nu_{\text{Cs}} \rightarrow \text{NaCs}^* + \hbar\nu_{\text{Na}} \rightarrow \text{NaCs}^+ + e^-$ and $\text{Na}(3S) + \text{Cs}(6S) + \hbar\nu_{\text{Na}} \rightarrow \text{Na}^*\text{Cs} + \hbar\nu_{\text{Cs}} \rightarrow \text{NaCs}^+ + e^-$ as shown in Fig. 2. The last steps are assumed to occur by autoionization into a bound state of the NaCs^+ molecule. This model is consistent with current calculations of the NaCs^+ energy levels. The ground-state asymptote of NaCs^+ dissociates into $\text{Cs}^+ + \text{Na}(3S)$ at 3.89 eV [10]. Predictions for the dissociation energy of the NaCs^+ molecular ion place it at 0.570 eV [11], 0.398 eV [12], or 0.210 eV [13] below this level, or at 3.32, 3.49, or 3.68 eV, respectively. The asymptotically doubly excited state of NaCs occurs at $\hbar\nu_{\text{Na}} + \hbar\nu_{\text{Cs}} = 3.53$ eV, making autoionization energetically possible according to two of the three predictions.

A series of two-color [14] spectroscopic studies was also carried out. In these experiments, either the Cs or the Na trap laser was extinguished for $20 \mu\text{s}$ at a repetition rate of ~ 5 kHz. During this $20 \mu\text{s}$ period, a frequency tunable probe laser (tuned near the wavelength of the extinguished trap laser) illuminates the atom cloud and a burst of NaCs^+ ions is produced. In Fig. 2(c), the probe was tuned near the Na trap transition and the Cs trap light was held fixed, while in the second experiment [Fig. 2(d)], the probe was tuned near the Cs transition and the Na trap light frequency was held fixed. The probe laser frequency was calibrated using (1) a wave meter (~ 100 MHz resolution), (2) a 20 GHz free spectral range $\ll 1$ MHz resolution scanning Fabry-Perot, (3) either a Cs or a Na saturated absorption spectrometer, and (4) the Na probe was referenced to known I_2 transitions. Because of the scheme used to cool and trap the Cs atoms, in steady state there is only a small number of atoms in the $\text{Cs}(F = 3)$ ground state (the population ratio $[F = 4/F = 3] \approx 5$). To improve the ion signal as the probe was scanned near the $\text{Cs}(F = 3)$ ground-state asymptote (i.e., from +4 to +12 GHz), an optical pumping cycle

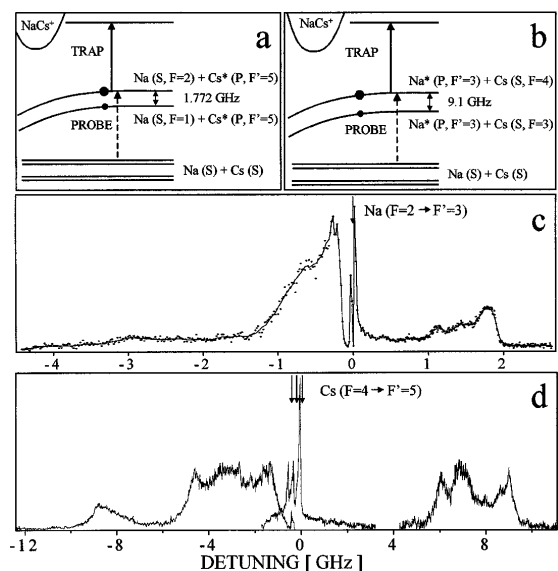


FIG. 2. NaCs^+ two-color PAI spectroscopy. (a) Proposed NaCs^+ PAI pathway with Cs (asymptotically) excited in the first step; (b) with Na excited in the first step. (c) Spectra taken with the probe laser tuned near the Na $D2$ line. (d) Spectra taken with probe tuned near the Cs $D2$ line. Arrows denote the hyperfine transitions of Cs. The holes burned in spectrum near zero detuning are due to the disruption of the trap by the probe. In (b), the probe laser was kept $\sim 30 \text{ mW/cm}^2$ to avoid power broadening (the width of the narrowest spectral structures did not depend on the probe laser power). In (c), different probe powers were used. From -2 to $+3.5 \text{ GHz}$, 100 mW/cm^2 was used, whereas, to improve the signal-to-noise ratio from -0.5 to -12 GHz , $\sim 3 \text{ W/cm}^2$ was used.

was used to increase the $\text{Cs}(F=3)$ population: $10 \mu\text{s}$ before the probe was applied, the diode laser repumper was detuned by $>20 \text{ GHz}$ while leaving the $6S_{1/2}(F=4) \rightarrow 6P_{3/2}(F'=5)$ Cs trap light on.

To interpret each of our spectra, both channels [Figs. 2(a) and 2(b)] must be considered. Consider the case where the probe laser is tuned to the blue ($\Delta > 0$) side of the Na (Cs) trapping transition. If the probe photon is the first photon [Fig. 2(a) for Cs probe light and Fig. 2(b) for Na probe light], then as Δ increases it passes from the Cs + $\text{Na}(F=2)$ [$\text{Na} + \text{Cs}(F=4)$] asymptote to the Cs + $\text{Na}(F=1)$ [$\text{Na} + \text{Cs}(F=3)$] asymptote causing a peak to appear when Δ equals the ground-state hyperfine splitting of the Na (Cs) partner [$\Delta_{\text{NaHF}} = 1.772 \text{ GHz}$ in Fig. 2(c) and $\Delta_{\text{CsHF}} = 9.125 \text{ GHz}$ in Fig. 2(d)]. These two peaks can also be understood in a picture where the trap photon is the first photon and the probe is the second photon. Here, the peaks occur as the probe passes from the $\text{Cs}^* + \text{Na}(F=2)$ [$\text{Na}^* + \text{Cs}(F=4)$] asymptote to the $\text{Cs}^* + \text{Na}(F=1)$ [$\text{Na}^* + \text{Cs}(F=3)$] asymptote. Unlike previous work on Na PAI, NaCs hyperfine features do not exhibit any blueshift [14]. In two-color Na PAI, a blueshift was attributed to a survival effect of the excited state against spontaneous emission. Here we observe no shift, suggesting that survival is less important in the

heteronuclear case. This is expected for heteronuclear collisions because initial excitation occurs at smaller R_{ex} and at a point where the slope in the potential is larger causing the atoms to accelerate more quickly. Both effects reduce the effects of survival.

One striking difference between Figs. 2(c) and 2(d) occurs on the red (low frequency) side of the peaks. In Fig. 2(c) this portion of the spectrum is characterized by a broad tapered tail as compared to the red side of the resonances in Fig. 2(d). To interpret this difference we consider the case where the first excitation is provided by the probe laser, representing a free-bound transition of the colliding ground-state pair into the rovibrational levels of the singly excited NaCs molecule. The long-range attractive interactions of a ground + excited colliding pair are described in Table I. There are three ground-state Hund's case (c) potentials of NaCs; 0^+ , 0^- , and 1. The C_6 coefficients for these have been calculated by several workers [15,16]. There are five excited-state long-range potentials for NaCs* and Na*Cs: 0^+ , 0^- , 1(2), and 2 [15,17] whose C_6 coefficients are also given [18]. From these values, the internuclear spacing R_{ex} , where the laser comes into resonance with the relevant ground and excited states, was calculated. Also shown are estimated vibrational level spacings near this point [18]. Notice that photoassociation of Na*Cs occurs at significantly closer range than for NaCs* and hence in a region of lower density of levels of the molecular intermediate.

Our spectra show a substructure with spacings $\sim 0.1\text{--}1 \text{ GHz}$. Splittings around the $\text{Na}(F=1 \rightarrow F') + \text{Cs}$ asymptote are identified as $\sim 300 \text{ MHz}$ while for $\text{Na}(F=2 \rightarrow F') + \text{Cs}$ there is at best some suggestion of features spaced by $\sim 700 \text{ MHz}$. Splittings in the NaCs* spectrum appear to be $\sim 300\text{--}400 \text{ MHz}$. These values are close to the vibrational spacings of the molecular states (see Table I). However, the structure of near dissociation PAI spectra is known to be complex [9] and has yet to be completely analyzed even for the homonuclear case, as dispersive forces and hyperfine structure [19] become relevant.

Figure 2(d) contains additional features: a peak at $\sim +7.4 \text{ GHz}$ which we attribute to a process in which the probe laser provides the first photon and the trap light the second photon: $\text{Na}(F=2) + \text{Cs}(F=3) + \hbar\nu_{\text{probe}} \rightarrow \text{Na}(F=1) + \text{Cs}^*(F=4,5) + \hbar\nu_{\text{Na}} \rightarrow \text{NaCs}^+ + e^-$. Here $\nu_{\text{probe}} = \nu_{\text{Cs}} + 9.1 \text{ GHz} - 1.77 \text{ GHz} = 7.4 \text{ GHz}$. Viewed as an excitation of free atoms, this should be forbidden; however, relaxation of atomic selection rules at small interatomic spacings can explain its appearance.

We have also measured the PAI rate constant $K_{\text{NaCs}^+}(I_{\text{Cs}}, I_{\text{Na}})$ defined as $d[\text{NaCs}^+]/dt = K_{\text{NaCs}^+} [\text{Na}][\text{Cs}]$, where $[A]$ denotes the concentration of species A. Figure 3 shows K_{NaCs^+} as a function of (a) the total Cs trap light intensity and (b) the total Na trap light intensity. We note that the observed saturation occurs at a lower I than for pure Na PAI and fine structure

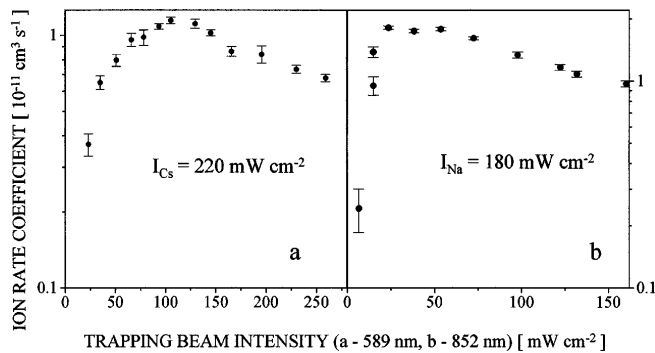


FIG. 3. The NaCs^+ rate coefficient $K_{\text{NaCs}^+}(I_{\text{Cs}}, I_{\text{Na}})$.

changing collision processes measured in Cs [20,21]. Again, this difference reflects the fact that the NaCs^* ($1/R^6$) interaction is of a shorter range than either the CsCs^* or NaNa^* ($1/R^3$) interactions. When the trap light intensity is greater than the I_{sat} of the atomic species, the temperature of the atoms is on the order of T_{Doppler} [22], and hence we estimate the total cross section for NaCs^+ production as $\sigma_{\text{NaCs}^+} = K_{\text{NaCs}^+}(I_{\text{Cs}}, I_{\text{Na}})v$, where v is the average Na-Cs thermal collision velocity. Taking v as the average of $T_{\text{Doppler-Na}}$ and $T_{\text{Doppler-Cs}}$, we find $\sigma_{\text{NaCs}^+} = 2.7 \times 10^{-13} \text{ cm}^2$ (for $I_{\text{Cs}} = 220 \text{ mW/cm}^2$ and $I_{\text{Na}} = 180 \text{ mW/cm}^2$). This cross section is comparable to that of PAI in trapped Na. We find this quite unexpected given the large difference in R_{ex} between the homonuclear and the heteronuclear cases.

In conclusion, we have observed the formation of NaCs^+ in a novel two-species MOT and presented a model for ion production in this heteronuclear system which we confirmed by studies of ion production as a function of laser intensity and frequency. The spectroscopy of ultracold heteronuclear collisions opens up new and exciting avenues of research in molecular spectroscopy and in the quest for ultracold molecular formation.

We are grateful to P.S. Julienne, W. Stwalley, and C. Williams for enlightening conversations. This work was supported by the National Science Foundation, the Packard Foundation, and the Army Research Office. J.P.S. is grateful for the support from a Horton Fellowship.

*Also with the Institute of Optics.

- [1] H. Wang *et al.*, *Z. Phys. D* **36**, 317 (1996); P.D. Lett, P.S. Julienne, and W.D. Phillips, *Annu. Rev. Phys. Chem.* **46**, 423 (1995), and references therein.

- [2] B. Bussery *et al.*, *J. Mol. Spectrosc.* **113**, 21 (1985); M. Movre and G. Pichler, *J. Phys. B* **10**, 2631 (1977); W. Stwalley *et al.*, *Phys. Rev. Lett.* **41**, 1164 (1978).
- [3] J. Shaffer and N.P. Bigelow, *Opt. Photonics News* **6**, 47 (1995); M.S. Santos *et al.*, *Phys. Rev. A* **52**, R4340 (1995).
- [4] H. Wang and W. Stwalley (to be published); M. Movre and R. Beuc, *Phys. Rev. A* **31**, 2957 (1985); B. Bussery *et al.*, *Chem. Phys.* **116**, 319 (1987); G. Igel-Mann *et al.*, *J. Chem. Phys.* **84**, 5007 (1986); M. Marinescu *et al.*, *Phys. Rev. A* **49**, 982 (1994); E. Lombardi and L. Jansen, *Phys. Rev. A* **33**, 2907 (1986). For higher temperature situations, see, for example, C. Gabbanini *et al.*, *Phys. Rev. A* **43**, 2311 (1991); C. Gabbanini *et al.*, *J. Phys. B* **24**, 3807 (1991).
- [5] R. Eisenschitz and F. London, *Z. Phys.* **60**, 491 (1930); G.W. King and J.H. Van Vleck, *Phys. Rev.* **55**, 1165 (1939).
- [6] M. Prentiss *et al.*, *Opt. Lett.* **13**, 452 (1988); D. Sesko *et al.*, *Phys. Rev. Lett.* **63**, 961 (1989); S.-Q. Shang *et al.*, *Phys. Rev. A* **50**, R4449 (1994).
- [7] V.S. Bagnato *et al.*, *Phys. Rev. A* **48**, R2523 (1993); P.D. Lett *et al.*, *Phys. Rev. Lett.* **67**, 2139 (1991).
- [8] We irradiated the pure Cs MOT with a strong laser ($I = 3 \text{ W/cm}^2$) at 589 nm (with only the Cs trapping light present, no ions of any kind are produced).
- [9] P.S. Julienne and R. Heather, *Phys. Rev. Lett.* **67**, 2135 (1991); R.W. Heather and P.S. Julienne, *Phys. Rev. A* **47**, 1887 (1993).
- [10] V.S. Letokhov, *Laser Photoionization Spectroscopy* (Academic Press, New York, 1987).
- [11] L. Bellemonte *et al.*, *J. Chem. Phys.* **61**, 3225 (1974).
- [12] L. Von Szentpaly *et al.*, *Chem. Phys. Lett.* **93**, 555 (1982).
- [13] A. Valance, *J. Chem. Phys.* **69**, 355 (1978).
- [14] V.S. Bagnato *et al.*, *Phys. Rev. Lett.* **70**, 3225 (1993).
- [15] M. Movre and R. Beuc, *Phys. Rev. A* **31**, 2957 (1985).
- [16] M. Marinescu *et al.*, *Phys. Rev. A* **49**, 982 (1994).
- [17] B. Bussery *et al.*, *Chem. Phys.* **116**, 319 (1987).
- [18] Vibrational splittings were calculated as $G(v) = D - \{(v_D - v)\overline{H}_n / [\sqrt{\mu} \sqrt{C_n}] \}^{2n/(n-2)}$. See R.J. Le Roy and R.B. Bernstein, *J. Chem. Phys.* **52**, 3869 (1970); R.J. Le Roy and R.B. Bernstein, *J. Mol. Spectrosc.* **37**, 109 (1971); W.C. Stwalley, *Chem. Phys. Lett.* **6**, 241 (1970). For entries N.A. in Table I, the above relation is not valid.
- [19] R.A. Frosch and H.M. Foley, *Phys. Rev.* **88**, 1337 (1952). Recently, a detailed study of hyperfine effects has been developed [C. Williams and P.S. Julienne, *J. Chem. Phys.* **101**, 2634 (1994)].
- [20] J. Shaffer *et al.* (to be published).
- [21] A. Fioretti *et al.*, *Phys. Rev. A* **55**, R3999 (1997).
- [22] We verified MOT temperatures by making linewidth measurements of the Doppler-free two-photon transition $3S_{1/2} \rightarrow 3P_{3/2} \rightarrow 4D_{5/2}$ Na transition.